CHAPTER - VI

PREPARATION AND CHARACTERIZATION OF Sb_2Se_3 THIN FILMS FROM NON - AQUEOUS MEDIUM

6.1 INTRODUCTION **113**

6.2 EXPERIMENTAL **113**

6.2.1 Thin film deposition **113**

6.2.1.1 Film preparation using SeO_2 **113**

6.2.1.2 Annealing of Sb_2Se_3 thin films **115**

6.2.1.3 Film preparation using $CSe(NH_2)_2$ **115**

6.2.2 CHARACTERIZATION OF Sb_2Se_3 THIN FILMS **116**

6.2.2.1 X-ray diffraction (XRD) **116**

6.2.2.2 Scanning electron microscopy (SEM) **116**

6.2.2.3 Optical absorption **116**

6.2.2.4 Electrical resistivity **116**

6.2.2.5 Thermoelectric power (TEP) **116**

6.3 RESULTS AND DISCUSSION **117**

6.3.1 X-ray diffraction (XRD) **117**

6.3.2 Scanning electron microscopy (SEM) **119**

6.3.3 Optical absorption **123**

6.3.4 Electrical resistivity **126**

6.3.5 Thermoelectric power (TEP) **128**

6.3.6 Annealing of Sb_2Se_3 thin films **128**

6.3.6.1 Films using SeO_2 **130**

6.3.6.1.1 X-ray diffraction (XRD) **130**

6.3.6.1.2 Scanning electron microscopy (SEM) **131**

6.3.6.1.3 Optical absorption **131**

6.3.6.1.4 Electrical resistivity **131**

6.3.6.1.5 Thermoelectric power (TEP) **132**

6.3.6.2 Films using $CSe(NH_2)_2$ **133**

REFERENCES **134**

6.1 INTRODUCTION

The amorphous thin films of Sb_2Se_3 are prepared by various technique [1 - 8] but no report is available on the preparation of polycrystalline Sb_2Se_3 thin films from a non - aqueous medium. The present chapter reports on the deposition of Sb_2Se_3 thin films from non - aqueous medium and study of their structural, optical and electrical properties. Effect of change of Se source on the film properties has also been discussed.

6.2 EXPERIMENTAL

Sb_2Se_3 thin films have been deposited by the spray pyrolysis technique, as discussed in section 3.2.1.1 and by using selenium dioxide [SeO_2] and selenourea [$CSe(NH_2)_2$] as Se source respectively.

6.2.1 Thin film deposition

Substrate cleaning

The substrate cleaning procedure discussed in section 3.1.2.2 is used to clean the glass substrates.

6.2.1.1 Film deposition using SeO_2

The initial ingredients used to prepare Sb_2Se_3 thin films are as follows :

i) A.R. Grade, antimony trichloride [$SbCl_3$] supplied by s.d. fine Chem., Limited, Boisar, Mumbai- 2.

ii) A.R. Grade, selenium dioxide [SeO_2] supplied by Qualigens Fine Chemicals, Mumbai.

iii) A.R. Grade, acetic acid glacial supplied by Qualigens Fine Chemicals, Mumbai.

iv) A.R. Grade, formaldehyde supplied by Qualigens Fine Chemicals, Mumbai.

The solutions of antimony trichloride ($SbCl_3$) and SeO_2 were prepared by dissolving the appropriate amount of the salts in acetic acid and formaldehyde, respectively. These equimolar solutions were mixed together in the appropriate volumes to obtain Sb : Se ratio as 2 : 3. The whitish turbidity resulted due to direct mixing of $SbCl_3$ and SeO_2 can be redisolved by the addition of express acetic acid (glacial). The orange coloured films were prepared by spraying the clear solution onto the preheated glass substrates.

Spray rate

During the Sb_2Se_3 film deposition the spray rate was maintained to be 14 cc min^{-1} [9].

Substrate temperature

A mixed solution of $SbCl_3$ and SeO_2 of concentration 0.1 M was sprayed with spray spray rate of 14 cc min^{-1} onto the set of glass substrates maintained at temperatures from 150 ^oC, at the interval of 25 ^oC, to 250 ^oC. The structural and electrical analyses of these films reveal that the as deposited films are amorphous in nature, while only the film deposited at 200^0 C and heat treated in N_2 atmosphere at 325 ^oC are polycrystalline. The electrical resistivity of these films has relatively higher conductivity as compared to the films deposited at other substrate temperatures and thus leads to the optimized substrate temperature [9].

Solution concentration

The Sb_2Se_3 thin films were prepared at solution concentration from 0.025 M to 0.1 M at optimised substrate temperature of 200 ^oC with spray rate of 14 cc min^{-1}. The structural and electrical characterization of annealed films show that the films deposited at concentration of 0.025 M are relatively higher crystalline and show relatively higher conductivity than the films prepared at other concentrations. 0.025 M is, therefore, taken as optimized solution concentration [10].

6.1.2.2 Annealing of the Sb_2Se_3 thin films

Annealing of Sb_2Se_3 thin films is carried out in N_2 atmosphere at temperature of 325^0 C for 2 hours as discussed in section 3.2.1.5.

6.2.1.3 Film preparation using selenourea [$CSe(NH_2)_2$]

Solutions of $SbCl_3$ and $CSe(NH_2)_2$ (A.R. Grade supplied by Qualigens Ltd.) were prepared in acetic acid (glacial). The equimolar solutions of $SbCl_3$ and $CSe(NH_2)_2$ were mixed together in appropriate volume to obtain Sb : Se ratio as 2:3. The films were prepared by spraying the mixed solution (28 cc) onto the preheated glass substrates. The spray rate was maintained at 3 cc min^{-1}. The substrate temperature and the solution concentration were optimized as 150^0 C and 0.01 M respectively [11]. The films were uniform, pinhole free, adherent and blackish brown in colour.

6.2.2 CHARACTERIZATION OF Sb_2Se_3 THIN FILMS

The Sb_2Se_3 films prepared using SeO_2 and $CSe(NH_2)_2$ at their respective optimized parameters were characterized by using X- ray diffraction (XRD), scanning electron microscopy, optical absorption, dark resistivity and TEP measurement techniques.

6.2.2.1 X - ray diffraction (XRD)

XRD studies were carried out as discussed in section 3.2.2.1.

6.2.2.2 Scanning electron microscopy (SEM)

SEM studies were carried out as discussed in section 3.2.2.2.

6.2.2.3 Optical absorption

To carry out the optical absorption studies the procedure discussed in section 3.2.2.3 was adopted.

6.2.2.4 Electrical Resistivity

To study the electrical characterisation of the films, dark resistivity measurements were carried out using two point d.c. probe method in the temperature range 300 to 500K. The details of experimental setup are discussed in Section 3.2.2.4.

6.2.2.5 Thermoelectric power (TEP)

The details of the experimental setup of TEP are given in section 3.2.2.5.

6.3 RESULTS AND DISCUSSION

In a spray pyrolysis method, the thermal energy for the decomposition and subsequent recombination of the species and the sintering and recrystallisation of the crystallites, is provided by the hot substrates. It is different for the different materials and the solvents used in the deposition process. Therefore the decomposition temperatures for Sb_2Se_3 thin films are different for two different Se sources and two different solvents, e.g. for SeO_2 source in aqueous medium, it is 300^0 C (Chapter V), for $CSe(NH_2)_2$ source in aqueous medium, it is 275^0 C (Chapter V), for SeO_2 source in non-aqueous medium, it is 200^0 C and for $CSe(NH_2)_2$ source in non - aqueous medium, it is 150^0 C.

The thickness of the prepared films was determined using relation 2.1. The density of deposited material is taken to be 5.81 gm cc^{-3} [12]. The thickness of the Sb_2Se_3 films deposited using SeO_2 and $CSe(NH_2)_2$ were found to be 1.3 μm and 0.52 μm respectively.

6.3.1 X-ray diffraction (XRD)

XRD patterns of Sb_2Se_3 thin films prepared using two different Se sources are studied in order to reveal their structural aspects.

Films using SeO_2

The appearance of the broad X-ray spectrum, as shown in Fig. 6.1 (a) for the films suggests the amorphous nature of the deposited material.

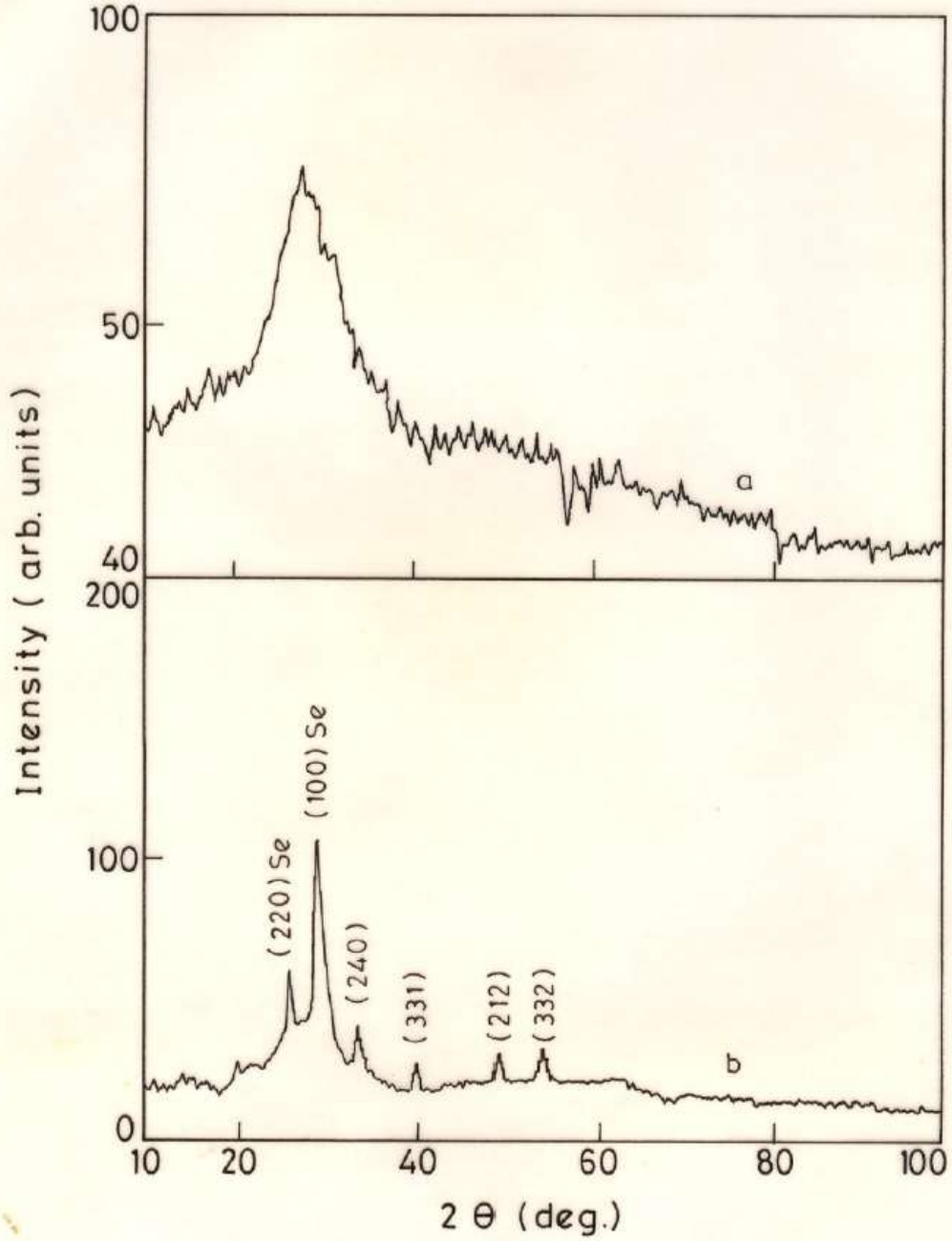

Fig. 6.1 : XRD patterns for the Sb_2Se_3 thin films prepared using SeO_2 ; a) as-deposited and b) annealed.

Films using $CSe(NH_2)_2$

Fig. 6.2 shows the XRD pattern for the Sb_2Se_3 films prepared using $CSe(NH_2)_2$ as a Se source from non - aqueous medium. The films are found to be amorphous in nature [11].

The structural difference between the Sb_2Se_3 films prepared using $CSe(NH_2)_2$ from aqueous (Chapter V) and non-aqueous media is due to the difference in stoichiometric proportion occurred; certainly due to the difference in reaction mechanisms, during pyrolytic decomposition of the Sb_2Se_3.

6.3.2 Scanning electron microscopy

Films using SeO_2

SEM micrographs of Sb_2Se_3 thin films deposited from non- aqueous medium onto glass substrates are studied to see the surface morphology of the film. SEM micrographs of as- deposited Sb_2Se_3 thin films are shown in Figs. 6.3 (a) and (b) for two different magnifications 2000x and 5000x respectively. The micrographs show the total coverage of the substrate by the film with rough surface morphology .

Films using $CSe(NH_2)_2$

SEM micrographs of as-deposited Sb_2Se_3 films prepared using $CSe(NH_2)_2$ are shown in Figs 6.4 (a) and (b) at two magnifications 2000x and 5000x respectively. The micrographs show holes at 5000x magnification. Incomplete decomposition of the particles at the film surface is also seen.

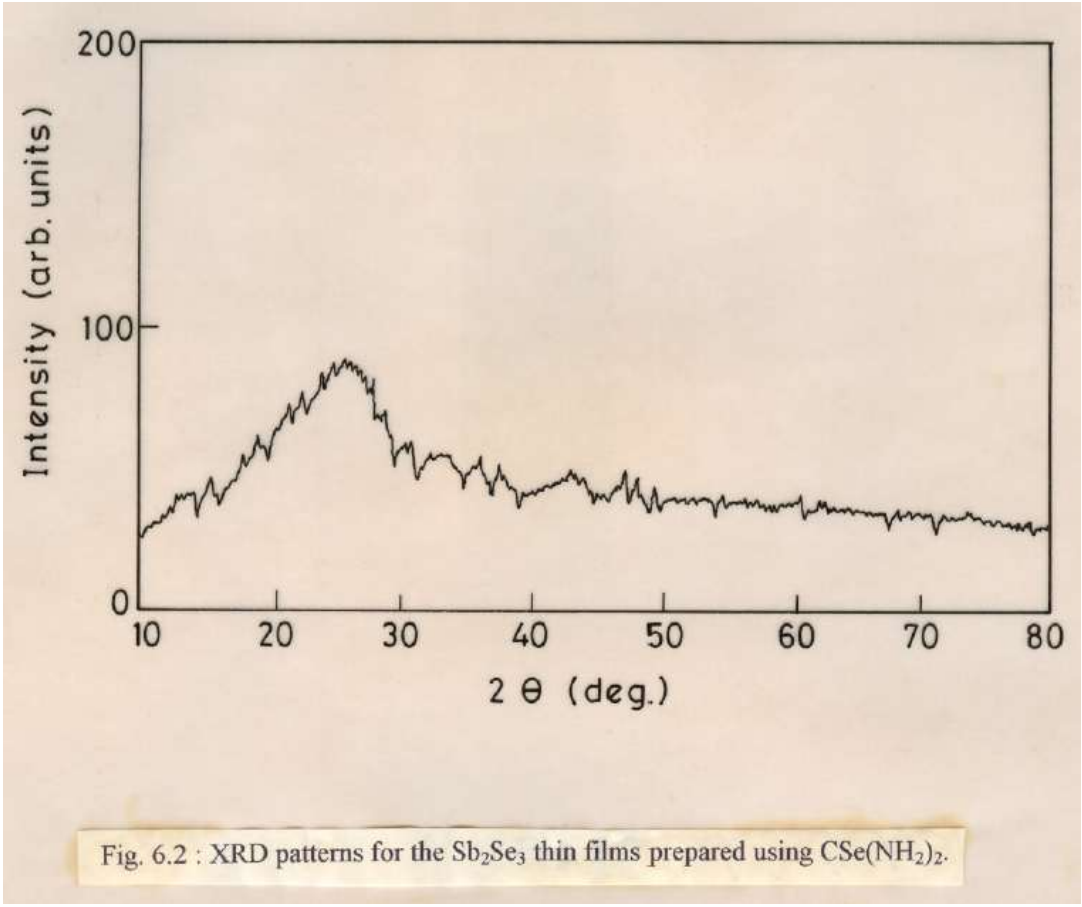

Fig. 6.2 : XRD patterns for the Sb_2Se_3 thin films prepared using $CSe(NH_2)_2$.

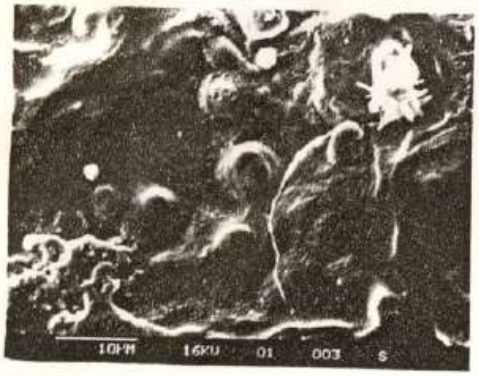

a)

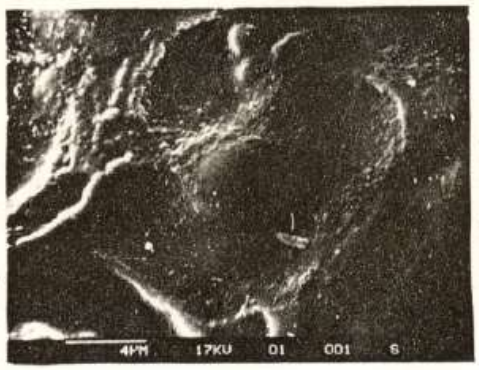

b)

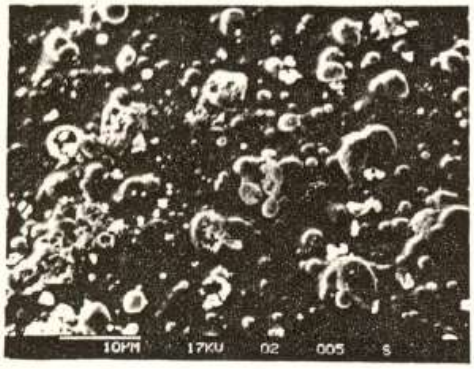

c)

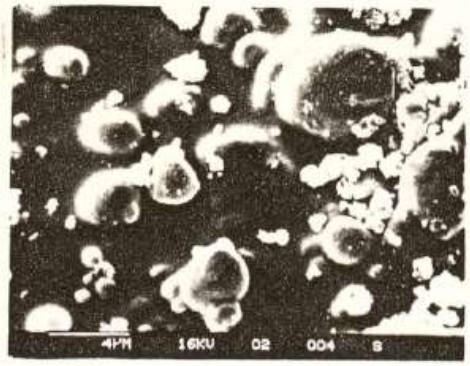

d)

Fig. 6.3 : SEM micrographs for Sb_2Se_3 thin films prepared from non-aqueous medium using SeO_2 as- deposited; at magnifications a) 2000x, b) 5000x and annealed; c) 2000x, b) 5000x

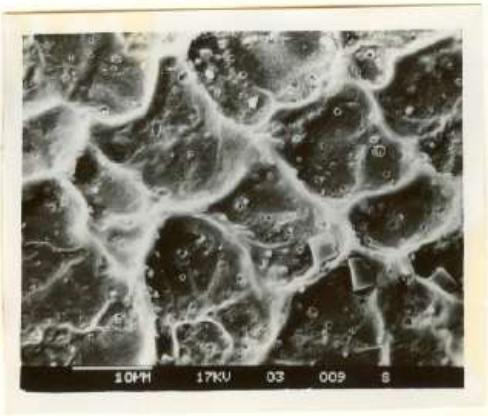

a)

b)

Fig. 6.4 : SEM micrographs for Sb_2Se_3 thin films prepared from non-aqueous medium using $CSe(NH_2)_2$ at magnifications a) 2000x and b)5000x

6.3.3 Optical absorption

The Sb_2Se_3 films prepared using two different Se sources from non-aqueous medium are optically characterized by measuring the optical density in the wavelength range of 300 to 1200 nm.

Films using SeO_2

Variation of optical density (αt) with wavelength (λ) for Sb_2Se_3 films is shown in Fig. 6.5. α is found to be of the order of 10^4 cm^{-1}. The energy dependent absorption coefficient can be expressed by the relation 2.8 for amorphous semiconductors [13 - 14] with n=2.

The absorption of photon energy for amorphous films of Sb_2Se_3 have been explained by many workers [1-4, 6-7]. Figure 6.6 (a) shows the plot of $(\alpha h\nu)^{1/2}$ versus $h\nu$ for as deposited film of Sb_2Se_3 prepared using SeO_2. The optical gap, obtained by extrapolating the straight line portion of the plot to energy axis at α=0, is found to be 0.86 eV. The difference in the value of optical gap observed and reported earlier [2] may be attributed to the different mechanisms of film formation.

Films using $CSe(NH_2)_2$

Variation of optical density (αt) with wavelength (λ) for Sb_2Se_3 films is shown in Fig. 6.7. α is of the order of 10^4 - 10^5 cm^{-1}. The exponential form of the tail, being observed, may be due to disorder and defects (e.g., gap states) in the amorphous material [9].

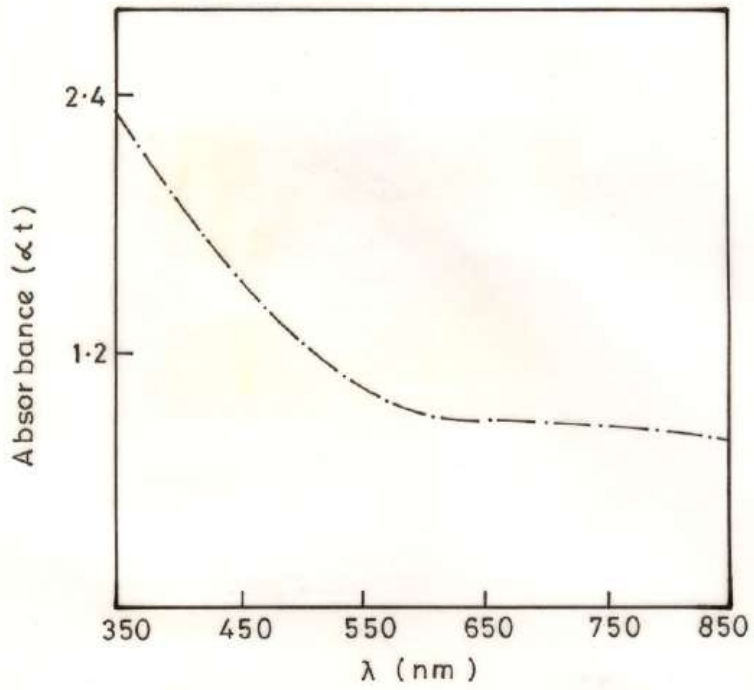

Fig. 6·5 – Variation of ∝t with λ for Sb_2Se_3 film prepared using SeO_2.

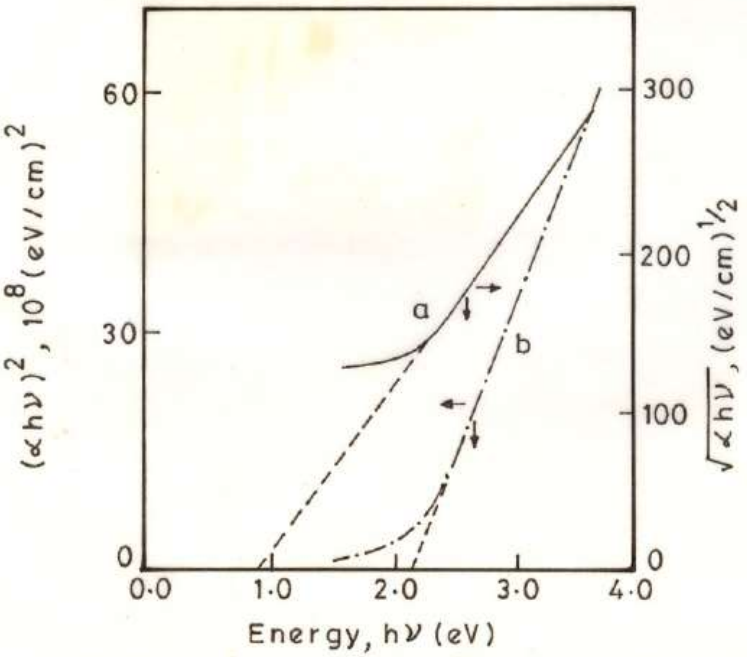

Fig. 6·6 – Plot of $(\alpha h\nu)^{1/2}$ and $(\alpha h\nu)^2$ versus $h\nu$ for Sb_2Se_3 thin films prepared using SeO_2,
a) as-deposited b) annealed.

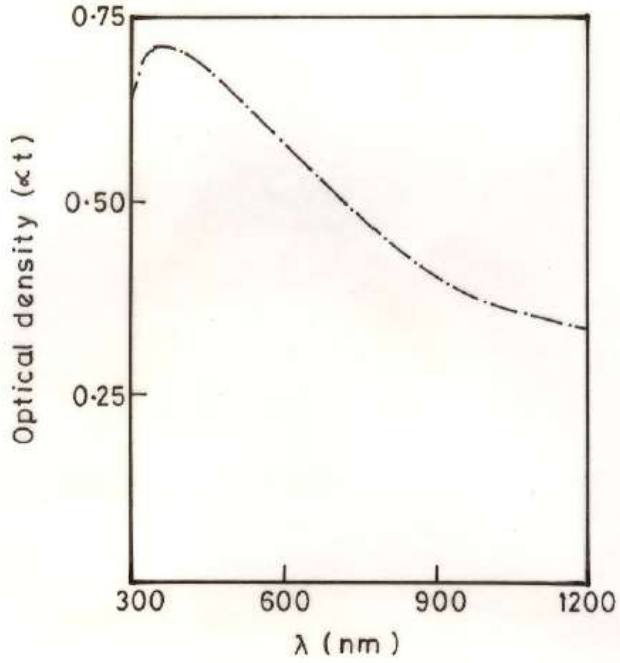

Fig.6·7 – Variation of ∝t with λ for Sb_2Se_3 thin film prepared using $CSe(NH_2)_2$.

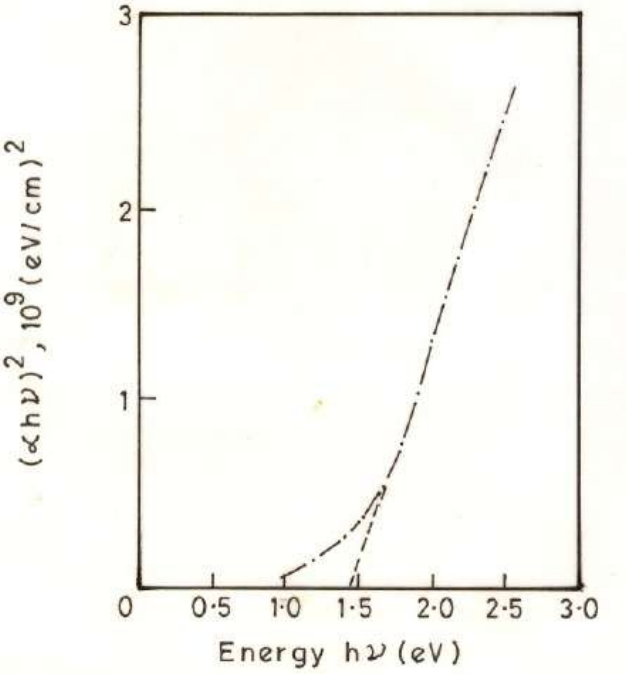

Fig. 6·8 – Plot of $(\alpha h\nu)^2$ versus $h\nu$ for Sb_2Se_3 thin films prepared using $CSe(NH_2)_2$.

The absorption coefficient at absorption edge follows the relation 2.8 for amorphous semiconductor [13,14] with n=2, but for the films prepared using $CSe(NH_2)_2$, α follows the relation 2.8 with n = 1/2. The plot of $(\alpha h\nu)^2$ versus $h\nu$ is linesr and is shown in Fig. 6.8. The observed optical gap is 1.45 eV [15] due to direct band transition. The difference in the optical gap of Sb_2Se_3 films using two different Se sources is attributed to the different decomposition temperatures and difference in density of gap states.

6.3.4 Electrical resistivity

Two point d.c. dark resistivity measurements show that the films prepared using SeO_2 and $CSe(NH_2)_2$ are highly resistive. The room temperature dark resistivity for both the films is of the order of 10^6 - 10^7 Ω.cm, similar to the result of others [3]. The high resistivity of the film may be due to discontinues, large grain boundaries and low thickness of the films.

Films using SeO_2

The variation of log (ρ) with reciprocal of temperature for the as - deposited films is depicted in Fig. 6.9 (a). It has been seen that the resistivity decreases with increase in temperature and supports for the semiconducting nature of the films. The calculated activation energy for the films was 0.77 eV [9].

Films using $CSe(NH_2)_2$

The variation of log (ρ) with 1000 /T for Sb_2Se_3 films deposited using $CSe(NH_2)_2$ is depicted in Fig. 6.10. Calculated activation energy for the films

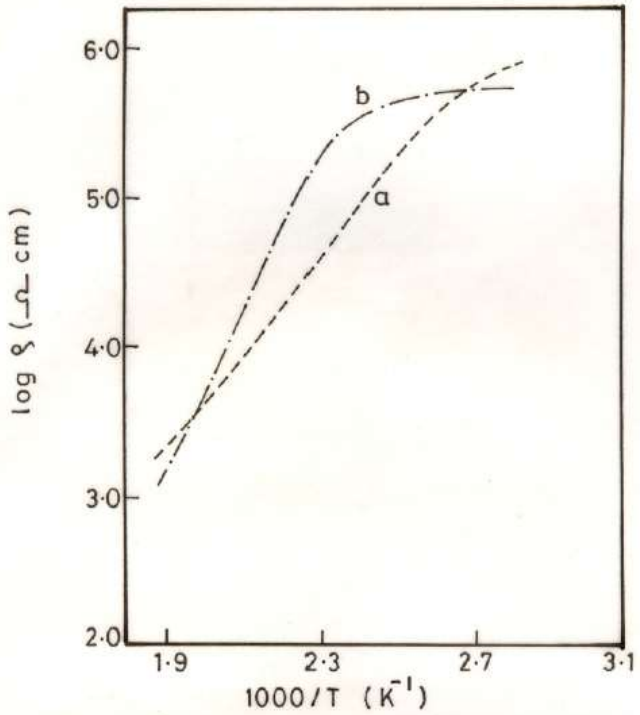

Fig. 6·9 – Variation of log ρ against 1000/T for Sb_2Se_3 thin films prepared using SeO_2 ; a) as-deposited b) annealed.

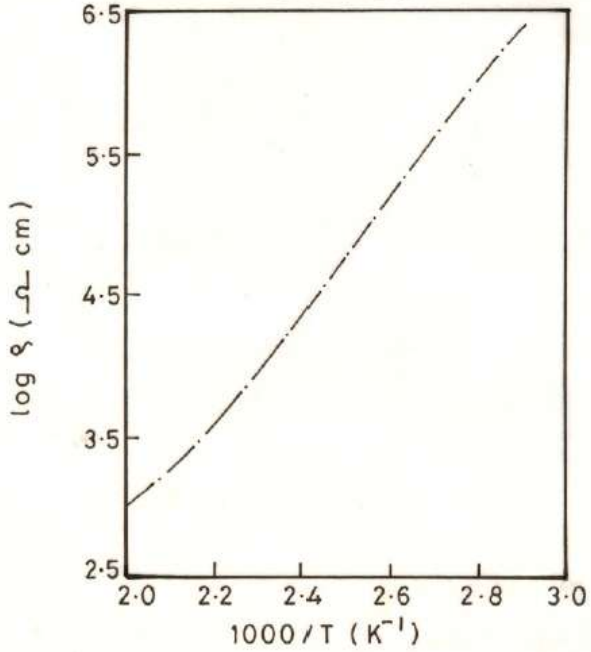

Fig. 6·10 – Variation of log ρ against 1000/T for Sb_2Se_3 thin films prepared using $CSe(NH_2)_2$.

is 0.82 eV. The difference in observed activation energies in two cases may be due to difference in stiochiometry of the material.

6.3.5 Thermoelectric Power (TEP)

It is seen that the polarity of thermally generated voltage is negative towards hot end indicating that the Sb_2Se_3 films prepared using SeO_2 and $CSe(NH_2)_2$ are of *p* - type conductivity.

Films using SeO_2

The dependence of thermoelectric e.m.f. on temperature difference is depicted in Fig. 6.11 (a). It is seen that e.m.f, first rises sharply upto the temperature difference of 30^0 C and varies linearly within 30 - 120^0 C, tending towards saturation.

Films using $CSe(NH_2)_2$

Fig. 6.12 shows the variation of thermo emf with temperature difference for the films prepared using and $CSe(NH_2)_2$. It is seen that the the emf varies linearly with temperature difference upto 100^0 C

The difference in observed variation of emf in two cases is due to difference in the carrier concentration and mobility in two cases.

6.3.6 Annealing of the Sb_2Se_3 thin films

The Sb_2Se_3 films were annealed in N_2 atmosphere for a optimized time of 2 hours at an optimized temperatures of 325 ^oC, to study its effect on their structural, optical and electrical properties.

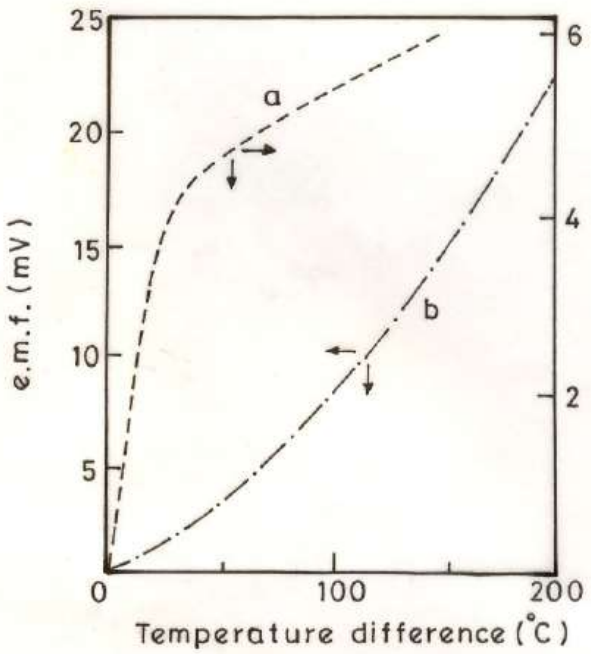

Fig. 6·11 – e.m.f. versus temperature difference for Sb_2Se_3 thin films prepared using SeO_2.
a) as-deposited b) annealed.

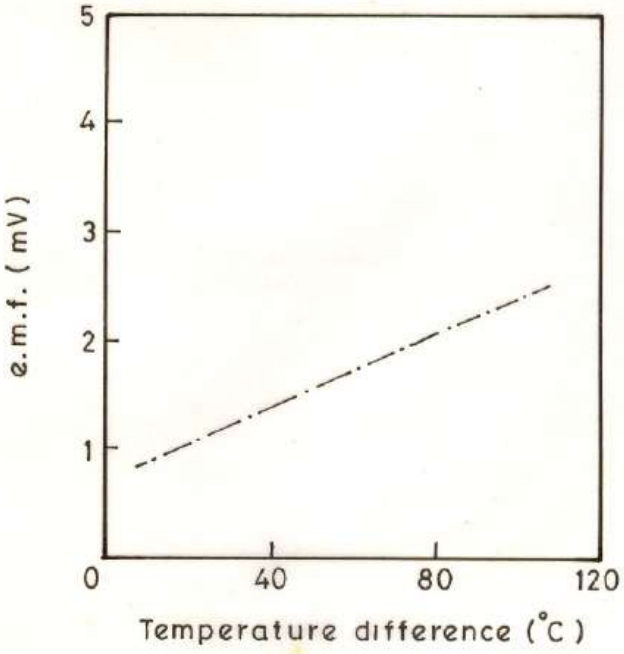

Fig. 6·12 – e.m.f. versus temperature difference for Sb_2Se_3 thin films prepared using $CSe(NH_2)_2$.

6.3.6.1 Films using SeO_2

6.3.6.1.1 X-ray diffraction

The XRD patterns of the annealed films show that the films are polycrystalline [Fig. 6.1 (b)]. Comparison of ASTM data [15] of Sb_2Se_3 with the observed data of the films reveals that the observed *d* values match with the standard *d* values. This confirms the formation of Sb_2Se_3 material. Table 6.2 shows the comparison of the standard *d* with ASTM data.

Table 1 comparison of the observed d values of Sb_2Se_3 thin films with standard ASTM data

Observed *d* values (Å)	Standard *d* values (Å)	I / Io (%)	(*hkl*) planes
3.437	3.416	39.43	(220) Se
3.033	3.03	100.00	(100) Se
2.646	2.629	23.83	(240)
2.229	2.238	19.52	(331)
1.858	1.861	28.61	(212)
1.699	1.698	26.18	(322)

Annealing promotes fusion of small crystallites (agglomerisation), thus reducing the grain boundary area, leads to the increase in grain size of the Sb_2Se_3 particles.

The calculated lattice constants are found to be a = 11.1881 Å, b = 11.2140 Å and c = 4.0348 Å [10] for orthorhombic crystal structure. These

values are very close to the values of lattice constants reported for single crystals of Sb_2Se_3 [17].

6.3.6.1.2 Scanning electron microscopy (SEM)

Fig. 6.3 (c) and (d) show the SEM micrographs of annealed Sb_2Se_3 films at two different magnifications 2000x and 5000x exhibiting its microstructure. Random distribution of particles having different size are observed. The film is continuos with fine grains. Surface is rough with presence of extra particles.

6.3.6.1.3 Optical absorption

The nature of the optical transition involved, for the polycrystalline film, can be determined by considering the dependence of α on $h\nu$ in equation 2.8 with n = 1/2.

In the present case the plot of $(\alpha h\nu)^2$ vs. $h\nu$ [Fig. 6.6 (b)] is linear, indicating that the transition is a direct one. The optical band gap Eg^{opt} is 2.14 eV due to direct transition has been observed [9]. However, for the as-deposited (amorphous) films, the optical band gap is obtained by plotting $(\alpha h\nu)^{1/2}$ versus $h\nu$ has been found to be 0.86 eV. This change in optical gap after annealing of the film at specific temperature may be due to (i) the change in atomic order in the amorphous phase and (ii) occurrence of 'wrong bonds' due to presence of 5-fold ring in amorphous structure [18].

6.3.6.1.4 Electrical resistivity

The dark resistivity for the annealed film is found to be of the order of 10^6 - 10^7 Ω.cm which is same as that of the amorphous film. The plot of log

(ρ) versus 1000/T for annealed film is shown in Fig. 6.9 (b). It is seen that there are two regions corresponding to low and high temperatures and electrical conduction in these films can take place via two parallel mechanisms : (a) Intrinsic conduction mechanism which occurs at high temperature (above 435 K) and (b) the hoping conduction in localized states at low temperatures (below 435 K) [7]. The activation energies corresponding to the low and high temperature regions are 0.52 eV and 0.01 eV, respectively. The activation energy in high temperature region is nearly similar to the reported value [7]. However, the decrease in activation energy in low temperature region (below 435 K) for polycrystalline film indicates that the deep trapping levels have been removed by annealing the samples [19].

6.3.6.1.5 Thermoelectric Power (TEP)

It has been found that the annealed Sb_2Se_3 films are of *p*-type conductivity. The dependence of thermo e.m.f. on temperature difference is shown in Fig. 6.11 (b) which varies linearly with the temperature difference. This is attributed to the increase in carrier concentration and mobility of the charge carriers with rise in temperature.

The difference in the nature of variation in the thermally generated voltage with temperature difference for ploycrystalline and amorphous films may be attributed to the relatively more ordered structure of the polycrystalline films than amorphous ones.

6.3.3.2 Films using $CSe(NH_2)_2$

Annealing of Sb_2Se_3 thin films is carried out at temperature of 300^0 C in N_2 atmosphere for 2 hours to see the effect of annealing on the structure of the films. It is observed that there is no change in the structure of amorphous Sb_2Se_3 thin films prepared using $CSe(NH_2)_2$ from non-aqueous medium. This may be due to non stiochiometry of the deposited material.

REFERENCES

1. C. Wood, L.R. Gilbert, R. Muller and C.M. Garner, J. Vac. Sci. Technol., 10 (1973) 739.
2. C. Wood, L.R. Gilbert, V. Van Pelt and B. Wolffing , phys. stat. sol. (b), 68 (1975) K39.
3. P. Pramanik and R.N. Bhattacharya, J. Solid State Chem., 44 (1982) 425.
4. L. Tichy and A. Triska, Solid State Commun., 41 (1982) 751.
5. P.S. Nikam and R.R. Pawar, Bull. Mater. Sci., 13 (1990) 343.
6. H.A. Zayed, A.M. Abo - Elsoud, A.M. Ibrahim and M.A. Kenaway, Thin Solid Films, 247 (1994) 94.
7. H.A. Zayed, A.M. Abo - Elsoud, B.A. Mansour and A.M. Ibrahim, Ind. J. Pure and Appl. Phys., 32 (1994) 334.
8. P.S. Nikam and H.S. Aher, Ind. J. Pure and Appl. Phys., 34 (1996) 393.
9. K.Y. Rajpure, C.D. Lokhande and C.H. Bhosale, Thin Solid Films, 311 (1997) 114.
10. K.Y. Rajpure and C.H. Bhosale, Symposium on Current Status on Solar Energy Materials and Systems, Anna University, Chennai, Feb. 24 - 25, 1997.
11. K.Y. Rajpure, C.D. Lokhande and C.H. Bhosale, Mater. Res. Bull., 34 (1999) .
12. J.C. Bailar and H.J. Emelens, Comprehensive Inorg. Chem., Oxford, (1973), p. 616.

13. N.F. Mott, E.A. Davis, Electronic Processes in Non - Crystalline Materials, 2nd edn., Clavendon Press, Oxford, (1979), p. 287.
14. S. Kondo, phys. status sol. (a), 153 (1996) 529.
15. K.Y. Rajpure, C.D. Lokhande and C.H. Bhosale, Turkish J. Phys., (1998) (Submitted).
16. ASTM data card file Nos. 15 - 861, 27 - 602 and 24 - 714.
17. G.P. Voutsas, A.G. Papazoglou, P.J. Rentzeperis and D. Sipkas, Z. Kristallograp., 171 (1985) 261.
18. G.A.N. Connel, W. Gaul, J. Non - Cryst. Solids, 8 - 10 (1972) 215.
19. K.M. Gadhave, P.P. Hankare, C.D. Lokhande, Ind. J. Pure and Appl. Phys., 32 (1994) 222.